Regional aerobic glycolysis in the human brain

S. Neil Vaishnavi[a], Andrei G. Vlassenko[a], Melissa M. Rundle[a], Abraham Z. Snyder[a,b], Mark A. Mintun[a,c], and Marcus E. Raichle[a,b,c,d,1]

Departments of [a]Radiology, [b]Neurology, [d]Anatomy and Neurobiology, and [c]Biomedical Engineering, Washington University, St. Louis, MO 63110

Contributed by Marcus E. Raichle, August 9, 2010 (sent for review July 28, 2009)

Aerobic glycolysis is defined as glucose utilization in excess of that used for oxidative phosphorylation despite sufficient oxygen to completely metabolize glucose to carbon dioxide and water. Aerobic glycolysis is present in the normal human brain at rest and increases locally during increased neuronal activity; yet its many biological functions have received scant attention because of a prevailing energy-centric focus on the role of glucose as substrate for oxidative phosphorylation. As an initial step in redressing this neglect, we measured the regional distribution of aerobic glycolysis with positron emission tomography in 33 neurologically normal young adults at rest. We show that the distribution of aerobic glycolysis in the brain is differentially present in previously well-described functional areas. In particular, aerobic glycolysis is significantly elevated in medial and lateral parietal and prefrontal cortices. In contrast, the cerebellum and medial temporal lobes have levels of aerobic glycolysis significantly below the brain mean. The levels of aerobic glycolysis are not strictly related to the levels of brain energy metabolism. For example, sensory cortices exhibit high metabolic rates for glucose and oxygen consumption but low rates of aerobic glycolysis. These striking regional variations in aerobic glycolysis in the normal human brain provide an opportunity to explore how brain systems differentially use the diverse cell biology of glucose in support of their functional specializations in health and disease.

blood flow | glucose consumption | metabolism | oxygen consumption | positron emission tomography

When glucose metabolism exceeds that used for oxidative phosphorylation despite sufficient oxygen to metabolize glucose to carbon dioxide and water, it has traditionally been referred to as aerobic glycolysis. Aerobic glycolysis has a long history in cancer cell biology, where the phenomenon was first noted by Otto Warburg (1), for whom it is often referred to as the "Warburg effect." Since Warburg's early work (2), much research has focused on the reasons for aerobic glycolysis mainly in cancer cells (3–5). Topics have included, but are not limited to, the role of aerobic glycolysis in biosynthesis, the maintenance of cellular redox states, the regulation of apoptosis and the provision of ATP for membrane pumps and protein phosphorylation. Little attention has been paid to the normal brain in this regard, despite the well documented presence of aerobic glycolysis (6–8; noteworthy recent exception in ref. 9).

From a whole-brain perspective, aerobic glycolysis may account for ~10–12% of the glucose used in the adult human (6–8). This percentage varies in interesting ways. In the newborn, it represents more than 30% of the glucose metabolized (10). In the adult, aerobic glycolysis varies diurnally from a low in the morning of ~11% to nearly 20% in the evening (7). In none of these observations do we have any information on the regional distribution of aerobic glycolysis in the brain or its role in cell biology.

The only information presently on regional brain aerobic glycolysis relates to task-induced changes in brain activity. Aerobic glycolysis has been observed locally to increase in the human brain during task-induced increases in cellular activity (11–13). Research on this activity-induced increase in aerobic glycolysis has focused on the mechanism by which glutamate is moved with sodium into astrocytes from the synapse. Findings strongly implicate membrane-bound, astrocyte Na^+/K^+ ATPase (14), which relies on glycolysis for the energy needed to remove the accumulated sodium from the astrocytes.

The experiments reported herein seek to expand our understanding of the role of glycolysis in the resting activity of the adult human brain by determining whether regional variations in glycolysis exist and how these regional variations might relate to regional variations in overall brain energy consumption. We were particularly interested to determine whether known functional specializations among brain areas are reflected in their use of aerobic glycolysis.

Results

Measures of Resting Oxygen and Glucose Metabolism. The cerebral metabolic rate for oxygen ($CMRO_2$) and cerebral metabolic rate for glucose (CMRGlu) as well as the cerebral blood flow (CBF) were imaged with PET in 33 normal right-handed adults in the resting awake state with eyes closed. Regional CMRGlu was measured using [^{18}F]-labeled fluorodeoxyglucose (FDG). Regional $CMRO_2$ was measured using a total of three scans involving the administration of [^{15}0]-labeled water, carbon monoxide, and oxygen. In each individual, regional $CMRO_2$ and CMRGlu were scaled to a whole-brain mean of 1 (local-to-global ratio; *Methods*). The individual results were averaged over subjects in a standard atlas space.

Aerobic glycolysis is traditionally assessed in terms of the molar ratio of oxygen consumption to glucose utilization [i.e., the so-called oxygen–glucose index (OGI)]. When all of the glucose metabolized is converted to carbon dioxide and water the OGI is 6. A number less than 6 indicates that aerobic glycolysis is present. In this study, we estimated aerobic glycolysis in this traditional manner by the voxelwise division of relative $CMRO_2$ by relative CMRGlu and scaling the resulting quotient imaging to obtain a whole-brain molar ratio of 5.323 based on earlier published work (6–8).

Although the OGI is a straightforward measure based on well-established metabolic principles, OGI images may be noisy in areas of low metabolism because they involve voxelwise division. Also, the value of the OGI is inversely related to the degree of aerobic glycolysis, a relationship sometimes confusing to readers. To overcome these limitations, we defined a previously uncharacterized measure of aerobic glycolysis in the brain: the glycolytic index (GI). The GI is obtained by conventional linear regression of CMRGlu on $CMRO_2$ (Fig. S1) and exhibiting the residuals scaled by 1000 (a procedure generally preferred for removal of covariates in contrast to ratio normalization). Positive

Author contributions: M.A.M. and M.E.R. designed research; S.N.V., A.G.V., and M.M.R. performed research; S.N.V., A.G.V., M.M.R., A.Z.S., M.A.M., and M.E.R. analyzed data; and S.N.V. and M.E.R. wrote the paper.

The authors declare no conflict of interest.

Freely available online through the PNAS open access option.

Data deposition: Data reported in this article have been deposited in the Central Neuroimaging Data Archive (https://cnda.wustl.edu/) (accession no. NP721).

See Commentary on page 17459.

[1]To whom correspondence should be addressed. E-mail: marc@npg.wustl.edu.

This article contains supporting information online at www.pnas.org/lookup/suppl/doi:10.1073/pnas.1010459107/-/DCSupplemental.

GI values represent more aerobic glycolysis and negative GI values represent less glycolysis than that predicted by the line of regression. The two measures of aerobic glycolysis, OGI and GI, are highly correlated in our data ($r = -0.913$, $P < 0.001$) (Fig. S1). For descriptive purposes, we will use the GI.

Following computation of GI maps for each subject, significance was assessed at the population level by voxelwise t tests against the null hypothesis of uniformly proportional glucose-to-oxygen metabolism, i.e., no deviation from the line of regression. The t maps were converted to equi-probable Z-maps and thresholded at $P < 0.0001$ ($Z > 4.4$, cluster >99 voxels) according to previously described methodology (15, 16).

Resting Aerobic Glycolysis. Regions with significantly elevated aerobic glycolysis were found bilaterally in prefrontal cortex, lateral parietal cortex, posterior cingulate/precuneus, lateral temporal gyrus, gyrus rectus, and caudate nuclei (Fig. 1 and Table 1). In contrast, significantly low aerobic glycolysis was found bilaterally in the inferior temporal gyrus and throughout the cerebellum.

Although the GI overall correlated to varying degrees with CBF and various metabolic measurements (Table 2), it is noteworthy that regional variations in $CMRO_2$, the primary measure of the brain's energy metabolism in this study, accounted for only 6% of the variance in aerobic glycolysis regionally. Clearly, factors other than brain work are contributing to the regional variations in aerobic glycolysis in the normal human brain. Data for all Brodmann regions are listed in Tables S1 and S2. Data for selected subcortical regions (Fig. S2) are listed in Table S3.

Brain Systems Exhibiting Elevated Aerobic Glycolysis. Examination of the GI map (Fig. 1 and Fig. 2*A*) suggested a correspondence between regions showing higher than average glycolysis and two distributed systems previously defined on the basis of functional neuroimaging studies, specifically, the default mode network (DMN) (17, 18) and additional areas in dorsolateral prefrontal and parietal cortices associated with task control processes (19–21). The DMN comprises brain regions that reliably reduce activity during the performance of goal-directed tasks (22). More recently, the DMN has been delineated by correlation mapping of spontaneous fluctuations of the blood oxygen level–dependent (BOLD) functional MRI (fMRI) signal acquired in the resting state (23, 24).

To delineate the DMN, we performed resting BOLD correlation mapping (25) in a subset ($n = 20$) of the present subjects. The DMN was mapped by conjunction analysis of the signals averaged over three nodes of the DMN (posterior cingulate [–5, –49, 40], left lateral parietal [–45, –67, 36], and medial prefrontal [–1, 47, –4] cortex). Similarly, the system associated with cognitive control and working memory was mapped using a distribution of seed regions placed bilaterally in prefrontal [–34, 51, 12], [24, 50, 13] and anterior parietal [–43, –55, 42], [48, –47, 42] cortex. Regions of significant BOLD correlations ($P < 0.01$, random effects analysis; $Z > 3.0$, cluster > 17) within the default and control systems are shown in Fig. 2 *B* and *C*, respectively. Figure 2*D* shows the overlap between regions of elevated aerobic glycolysis and a mask computed as above threshold in either the DMN or control system. These two distributed systems together account for most cortical areas showing high levels of aerobic glycolysis at rest.

Finally, we noted various apparent hemisphere asymmetries in both cortical and subcortical areas (Tables S1–S5). However, in the context of our entire data set, none of these apparent asymmetries are statistically significant when corrected for multiple comparisons. It therefore remains for future research to determine whether asymmetries do exist when examined in a hypothesis-driven, targeted approach.

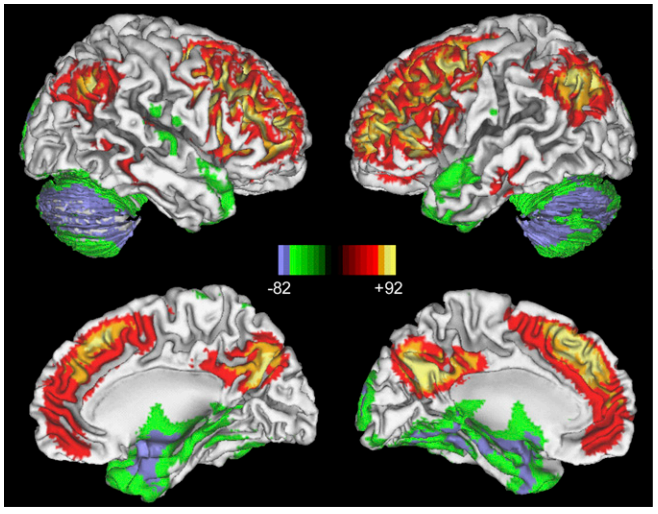

Fig. 1. Distribution of aerobic glycolysis in resting human brain using GI ($n = 33$, groupwise t test, $|Z|>4.4$, $P < 0.0001$, cluster > 99, corrected for multiple comparisons). Specifically, regions with significantly high glycolysis include bilateral prefrontal cortex, bilateral lateral parietal lobe, posterior cingulate/precuneus, gyrus rectus, bilateral lateral temporal gyrus, and bilateral caudate nuclei. In contrast, cerebellum and bilateral inferior temporal gyrus have significantly low levels of aerobic glycolysis.

Discussion

The regional variations in aerobic glycolysis in the normal human brain are striking (Fig. 1). The highest levels reside within two cortical systems, the DMN (17), which has come to be associated with a variety of self-referential functions (18) as well as a more fundamental role in the organization of brain function (26, 27); and areas in frontal and parietal cortex that have been associated with task control processes (19–21) (Fig. 2). As a counterpoint to brain systems with elevated aerobic glycolysis are areas with significantly reduced GI levels relative to the brain mean. Most prominent among these are the cerebellum and the hippocampal formation, an element of the DMN (23, 28). For future research the challenge will be to understand why levels of aerobic glycolysis vary so dramatically among brain systems. We examine the possibilities in terms of functions attributed to aerobic glycolysis, recognizing at the outset that few answers presently exist. Our objective is to identify opportunities for future work.

Energy. One factor responsible for ongoing aerobic glycolysis in the brain is likely to be the need to support membrane-bound, ATP-dependent processes. Best characterized in this regard is the process whereby glutamate is removed from the synapse into astrocytes along with sodium. The sodium is then returned to the extracellular fluid by Na^+/K^+-ATPase. The energy needed for the pumping action of Na^+/K^+-ATPase is derived from aerobic glycolysis (29, 30).

That glycolysis might supply ATP for membrane bound Na^+/K^+-ATPase is neither new nor restricted to the brain. Data from human red cell membranes (31), skeletal muscle (32), vascular smooth muscle (33), and neurons (34) all provide independent evidence in support of such a possibility. The use of aerobic glycolysis as a brain energy source may seem surprising because it is seemingly inefficient: glycolysis produces a net 2 ATP versus 30 ATP for complete oxidation to carbon dioxide and water. However, it produces ATP at a rate much faster than oxidative phosphorylation (35), making it uniquely suited to accommodate small, rapidly changing requirements in energy for Na^+/K^+-ATPase.

Because of the unique role of the astrocyte in using aerobic glycolysis for glutamate cycling, it is interesting to note that the ratio of neurons to nonneuronal cells can vary greatly in the hu-

Table 1. Regions with aerobic glycolysis, as determined by glycolytic index, significantly ($P < 0.0001$) different from line of regression ($n = 33$, groupwise t test, $Z > 4.4$, cluster >99, corrected for multiple comparisons) under the assumption of a homogenous normal bivariate distribution of $CMRO_2$ and CMRGlu

Region	Z score	AVG Z score	Coordinates	Volume (cm^3)	GI	OGI	$CMRO_2$	CMRGlu	CBF
Prefrontal cortex	9.30	6.30	[41, 13, 34]	271.36	102.74 ± 18.92	4.61 ± 0.11	1.07 ± 0.02	1.18 ± 0.02	1.10 ± 0.02
L lateral parietal	9.06	5.74	[–41, –61, 36]	33.17	85.55 ± 22.35	4.70 ± 0.16	1.10 ± 0.02	1.19 ± 0.03	1.06 ± 0.03
R lateral parietal	8.16	5.70	[47, –57, 40]	30.38	82.37 ± 26.97	4.71 ± 0.16	1.11 ± 0.03	1.19 ± 0.03	1.08 ± 0.03
Posterior cingulate	8.03	5.90	[1, –59, 24]	29.97	107.55 ± 29.18	4.73 ± 0.16	1.30 ± 0.04	1.39 ± 0.04	1.27 ± 0.03
Gyrus rectus	7.25	5.01	[31, 27, –14]	4.51	75.15 ± 32.94	4.76 ± 0.22	1.02 ± 0.04	1.08 ± 0.05	1.03 ± 0.05
R lateral temporal	6.30	4.94	[61, –35, –8]	6.85	66.45 ± 35.03	4.75 ± 0.20	1.10 ± 0.04	1.16 ± 0.05	1.06 ± 0.04
L lateral temporal	6.01	4.98	[–57, –31, –18]	5.26	64.88 ± 34.36	4.71 ± 0.24	1.02 ± 0.06	1.09 ± 0.06	1.00 ± 0.05
R caudate	5.95	5.09	[7, 9, 8]	1.34	78.45 ± 56.24	4.47 ± 0.32	0.84 ± 0.09	0.94 ± 0.11	0.86 ± 0.10
L caudate	5.65	4.89	[–11, 5, 16]	1.09	79.08 ± 61.48	4.55 ± 0.39	0.94 ± 0.10	1.04 ± 0.09	0.95 ± 0.09
L inferior temporal	–8.00	–5.74	[1, –11, –24]	26.89	–94.52 ± 22.88	5.67 ± 0.28	0.92 ± 0.04	0.83 ± 0.03	0.99 ± 0.04
R inferior temporal	–8.18	–5.94	[33, 5, –18]	32.86	–101.59 ± 21.21	5.70 ± 0.22	0.93 ± 0.03	0.83 ± 0.03	1.00 ± 0.03
Cerebellum	–8.98	–6.64	[1, –61, –22]	259.42	–143.46 ± 25.05	5.94 ± 0.23	1.04 ± 0.03	0.89 ± 0.03	1.06 ± 0.03

Data are shown as mean ± SD. Coordinates represent peak GI Z score location in Talairach system. CBF, cerebral blood flow; CMRGlu, cerebral metabolic rate of glucose; $CMRO_2$, cerebral metabolic rate of oxygen; GI, glycolytic index; L, left; R, right; AVG, average.

man brain (36). For example, the cerebral cortex contains ≈19% of the brain's neurons and nearly 72% of its nonneuronal cells, whereas in the cerebellum the percentages are reversed [i.e., 80% and 19%, respectively (36)]. This observation suggests that one of the factors contributing to the regional variation in aerobic glycolysis may be the percentage of nonneuronal cells. An analysis of the cerebral cortex with regard to regional variations in the ratio of neurons to nonneuronal cells would be most interesting particularly if it could identify the percentage of nonneuronal cells that are astrocytes.

A more extended view of the role of aerobic glycolysis in the generation of ATP has emerged from the observation that glycolytic enzymes are found in the postsynaptic density (PSD) (34), a very dynamic complex containing various ion channel proteins, synaptic receptors, and signal transduction pathways (37, 38) that are turning over and being replaced with half-lives of minutes, hours, days, or weeks (39). In the PSD, Na/K-ATPase has been identified as critical for AMPA receptor turnover (40). Na/K-ATPase dysfunction leads to a loss of cell-surface expression of AMPA receptors and a long-lasting depression in synaptic transmission (40). If one of the reasons for positioning glycolytic enzymes in the PSD is to fuel the Na/K-ATPase pump, then aerobic glycolysis assumes a critical role in synaptic plasticity.

With regard to the energy needs of the PSD, it should be noted that mitochondria are rarely seen in dendritic spines (41, 42) in contrast to axons (43), notwithstanding the fact that lac-

Table 2. Correlations over Brodmann regions between metabolic variables

Correlation	GI	OGI	$CMRO_2$	CMRGlu	CBF
GI	1	–0.986*	0.243**	0.690*	0.501*
OGI		1	–0.119	–0.591*	–0.384*
$CMRO_2$			1	0.869*	0.822*
CMRGlu				1	0.869*
CBF					1

CBF, cerebral blood flow; CMRGlu, cerebral metabolic rate of glucose; $CMRO_2$, cerebral metabolic rate of oxygen; GI, glycolytic index; OGI, oxygen-to-glucose index.
*$P < 0.001$.
**$P < 0.05$.

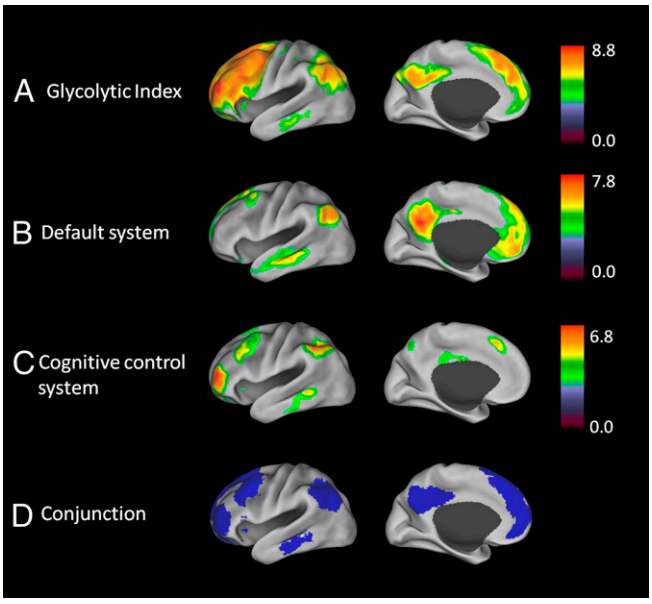

Fig. 2. Results of conjunction analysis between resting aerobic glycolysis using the GI and BOLD correlation maps of the default and cognitive control systems. (*A*) Regions with elevated aerobic glycolysis ($n = 33$, groupwise t test, $Z > 4.4$, $P < 0.0001$, cluster > 99, corrected for multiple comparisons). (*B*) Default system as delineated by BOLD correlation mapping ($n = 20$, groupwise t test, $Z > 3.0$, $P < 0.01$, cluster > 17, corrected for multiple comparisons). (*C*) Cognitive control system defined as in *B*. (*D*) Intersection of voxels showing significantly elevated GI and membership in either the default or cognitive control systems.

tate transporters designed to import lactate into dendritic spines as mitochondrial fuel are present (44). Reconciling such seemingly contradictory observations with the energy needs of dendritic spines presently is difficult. Regardless of the outcome it is important to note that aerobic glycolysis makes many other important contributions to the cell biology of the brain that may be equally important to the synapse. We review these next.

Biosynthesis. Glucose makes important contributions to anabolic processes in all organs of the body providing needed intermediates for cellular proliferation including NADPH, nucleotides for DNA replication (45), and intermediates for fatty acid synthesis (46, 47) all largely by way of the pentose phosphate pathway (PPP). In animal experiments, estimates of the amount of glucose entering the PPP in the mature brain have been variable but generally low (reviewed in ref. 48). Recent work in cultured neurons places this figure considerably higher because of an apparently low level of phosphofructokinase-2 (PFK-2) in neurons (49). PFK-2 is a key regulator of PFK-1, the gatekeeper of glycolysis (49). Could this difference between cultured neurons, usually harvested from immature animals, and in vivo measurements be a function of development, with maturity shifting glucose away from the PPP toward glycolysis?

Several lines of research provide a perspective from which to evaluate the above question. These include brain development and the sleep–wake cycle in adults. In the developing nervous system, aerobic glycolysis appears to play a substantial role, consistent with its potential to provide the building blocks for cell development and proliferation. In the preterm human infant, glycolysis accounts for more than 90% of the glucose consumed (50, 51). By term, 35% of the glucose consumed by the human infant represents aerobic glycolysis (10) compared with 10–12% in the adult (6, 8).

From term to adulthood, we have information only on the CMRGlu (52) preventing the assessment of aerobic glycolysis specifically during this critical developmental period. This is a serious void in our knowledge. Nevertheless, it is noteworthy that CMRGlu achieves adult levels by 2 y of age and continues to rise over the first decade to levels twice that of the adult (an astonishing increase if it truly represents oxidative phosphorylation, which seems unlikely) and then commences a gradual decline to adult levels by the early 20s (52). This trajectory in CMRGlu parallels the known overproduction of neuropil components followed by their pruning as the brain achieves adult status. Refining our understanding of just how glucose is used in this critical period of development should receive high priority in future research. The necessary data must come from parallel measurements of $CMRO_2$ and CMRGlu that are required for the quantification of aerobic glycolysis. Also of interest would be regional studies of the activity of enzymes critical for the control of the brain's intermediary metabolism during development. Although it is unlikely that such experiments will be conducted in humans, primate models of spinogenesis (53) provide an ideal model system for quantitative in vivo metabolic studies with PET and complementary studies of enzyme activity.

Data supporting the possible role of aerobic glycolysis in anabolic processes in the adult brain come from two sources. First, whole-brain studies of $CMRO_2$ and CMRGlu in humans reveal a diurnal variation in both $CMRO_2$, which is 20% higher, and CMRGlu, which is 38% higher, in the evening before sleep as compared with the next morning. From these data it can be estimated that aerobic glycolysis almost doubles during wakefulness. Second, Madsen et al. (54) reported a persistent resetting of the OGI (i.e., ~10% increase in aerobic glycolysis) following the performance of a demanding cognitive task. Together these two studies provide a tentative link between the metabolism of learning-induced biosynthesis and a hypothesis that associates wakefulness with synaptic potentiation and sleep with synaptic renormalization (55, 56), a process that has been associated with changes in brain glucose consumption in laboratory animals (57).

Redox States. Glucose plays an important role regulating the redox state of the brain. This occurs both during the production of ATP via glycolysis and also through the operation of the PPP. The importance of the redox state to energy production and the regulation of CBF via glycolysis has received considerable attention (see refs. 58 and 59 regarding the recent work on CBF), whereas the importance of glucose in regulating the redox state of the brain via the PPP has not. A recent paper (9) redresses this neglect by suggesting that glucose acting via the PPP inhibits apoptosis in both cancer cells and neurons by the redox inactivation of cytochrome *c*. The insight that this work provides is that both cancer cells and neurons achieve an adaptive advantage for long-term survival through management of their redox state via the PPP. Particularly interesting in this regard is the fact that areas of the normal human brain with elevated aerobic glycolysis (Fig. 1) are nearly identical with those that accumulate amyloid, and exhibit atrophy and disrupted metabolism in Alzheimer's disease as detailed in our companion paper (60) as well as elsewhere (61). This observation suggests to us that a loss of an adaptive advantage provided by aerobic glycolysis in brain systems that are particularly dependent upon it might be a critical component in the pathophysiology of Alzheimer's disease, a subject that we have previously explored in more detail (60).

In summary, we hope that our work will serve to stimulate the interest of the neuroscience community in the many critical functions glucose serves in the brain including, but not limited to, substrate for energy generation through glycolysis and oxidative phosphorylation. The opportunities for a deeper understanding of brain function in health and disease this affords seem plentiful.

Methods

Participants. A total of 33 healthy, right-handed neurologically normal participants (19 women and 14 men) aged 20–33 y (mean 25.4 ± 2.6 y) were recruited from the Washington University community. Subjects were excluded if they had contraindications to MRI, history of mental illness, possible pregnancy, or medication use that could interfere with brain function. All experiments were approved by the Human Research Protection Office and the Radioactive Drug Research Committee at Washington University in St. Louis. Written informed consent was provided by all participants.

Image Acquisition. MRI scans for structural and functional imaging were obtained on a 3-T Allegra scanner (Siemens), and all PET studies were performed on a Siemens model 961 ECAT EXACT HR 47 PET scanner (Siemens/CTI). Image acquisition details are available in *SI Text*.

General PET Data Analysis. We have assessed regional differences in resting $CMRO_2$, CMRGlu, and aerobic glycolysis in a manner independent of whole-brain quantitative measures. This strategy (*Methods*) differs somewhat from that originally described (11, 62–64) in which absolute rates for CMRGlu and $CMRO_2$ were determined. The primary advantage of the present strategy is its improved accuracy in determining the regional variations in $CMRO_2$ and CMRGlu. This is due to the elimination of rapid arterial blood sampling for the determination of an arterial input function for quantitative measurements of $CMRO_2$ and CMRGlu. Arterial blood sampling of rapidly time-varying radioactivity is an inherently noisy measurement that would have significantly compromised our ability to accurately assess levels of metabolism regionally. Because our primary interest was in regional variations in our measurements and not absolute values, we elected to forego arterial blood sampling in this study.

Preprocessing. For each subject, measures of CBF, cerebral blood volume, $CMRO_2$, and CMRGlu were aligned to each other and then to the subject's MRI scan [magnetization-prepared 180° radio-frequency pulses and rapid gradient-echo image (MP-RAGE)]. The realigned data were then transformed to atlas space using in-house software and scaled to a whole-brain mean of 1 (local-to-global ratio as in ref. 22). Our atlas representative target image represents Talairach space as defined by Lancaster et al. (65).

OGI. OGI was computed by a voxelwise division of $CMRO_2$ by CMRGlu to compute a local-to-global OGI. For comparison with traditional OGI measures, this ratio was scaled by 5.323 (6).

GI. To quantitatively assess aerobic glycolysis, we performed a linear regression of CMRGlu on $CMRO_2$. The residuals were scaled by 1,000 to produce the GI, which represents glucose consumption above or below that predicted by oxygen consumption.

PET statistics. To combine results across subjects, we computed a general linear model that contained metabolic data for $CMRO_2$, CMRGlu, CBF, OGI, and GI for each subject. We performed groupwise random effects analysis (one-sample *t* test; $n = 33$) to determine regions with significant deviations in their metabolic values from the whole-brain mean. Images were thresholded at a $Z > 4.4$ ($P < 0.0001$, cluster >99, corrected for multiple comparisons).

Surface mapping. Volumetric statistical results were projected onto the cortical surface of the PALS B12 (population-average landmark and surface-based) atlas by multifiducial mapping (66). Surface mapping was performed using CARET v5.512 (http://brainmap.wustl.edu/caret).

Brodmann regions. Brodmann regions were extracted from the PALS B12 atlas using CARET v5.512 (http://brainmap.wustl.edu/caret). Values for $CMRO_2$, CMRGlu, CBF, OGI, and GI were extracted for each Brodmann region in the brain (41 regions for each hemisphere) from the general linear model computed for each subject. Comparison of metabolic values between different Brodmann regions involved paired group wise *t* tests ($n = 33$, two-tailed $\alpha = 0.05$).

Correlations. Pearson product–moment correlations between metabolic values were performed over cortical Brodmann regions. Correlations were weighted by the size (number of voxels) of the Brodmann regions used. Weighted correlation across Brodmann regions is equivalent to voxelwise computation of the standard Pearson product–moment correlation after assigning to every voxel within a Brodmann region the value of its regional mean. Significance of correlations was computed using $\alpha = 0.05$ and 80 df. Statistical analysis was performed using SPSS for Windows v16.0 (SPSS Inc).

Subcortical regions. As CARET (http://brainmap.wustl.edu/caret) does not provide subcortical parcellations, regions of bilateral caudate, putamen, globus pallidus, and thalamus were manually drawn on our representative atlas MPRAGE using Analyze v6.1 (Mayo) as shown in Fig. S2 and presented in Table S3.

Default mode network and control system regions. Details of the seed-based, resting-state fMRI strategy used in the delineation of elements of these two systems are presented in Figs. S3 and S4. The results of this analysis are presented in Tables S4 and S5.

Conjunction analysis. A conjunction analysis was performed to qualitatively compare regions with elevated aerobic glycolysis measured via PET and the default and cognitive control systems delineated by resting-state fMRI correlation mapping (image acquisition section in *SI Text*). Z score maps of aerobic glycolysis were thresholded at a $Z > 4.4$ ($P < 0.0001$, cluster > 99 voxels, corrected for multiple comparisons). The conjunction image (Fig. 2*D*) was computed by identifying voxels showing significantly elevated aerobic glycolysis *and* being within either default *or* control systems (conjunction = GI significantly high Λ [voxel $\in$ default system **V** voxel $\in$ cognitive control system]).

ACKNOWLEDGMENTS. We thank Lenis Lich for many years of skilled technical assistance in PET imaging and Lars Couture and Russ Hornbeck for help with data processing and analysis. This work was supported by the National Institutes of Health Grants NS06833, NS057901, NS048056, and MH077967 and by a grant from the James S. McDonnell Foundation.

1. Warburg O, Posener K, Negelein E (1924) Uber den Stoffwechsel der Carcinomzelle. *Biochem Z* 152:309–344.
2. Warburg O, Wind F, Negelein E (1927) The metabolism of tumors in the body. *J Gen Physiol* 8:519–530.
3. DeBerardinis RJ, Lum JJ, Hatzivassiliou G, Thompson CB (2008) The biology of cancer: Metabolic reprogramming fuels cell growth and proliferation. *Cell Metab* 7:11–20.
4. Hsu PP, Sabatini DM (2008) Cancer cell metabolism: Warburg and beyond. *Cell* 134: 703–707.
5. Vander Heiden MG, Cantley LC, Thompson CB (2009) Understanding the Warburg effect: The metabolic requirements of cell proliferation. *Science* 324:1029–1033.
6. Raichle ME, Posner JB, Plum F (1970) Cerebral blood flow during and after hyperventilation. *Arch Neurol* 23:394–403.
7. Boyle PJ, et al. (1994) Diminished brain glucose metabolism is a significant determinant for falling rates of systemic glucose utilization during sleep in normal humans. *J Clin Invest* 93:529–535.
8. Powers WJ, et al. (2007) Selective defect of in vivo glycolysis in early Huntington's disease striatum. *Proc Natl Acad Sci USA* 104:2945–2949.
9. Vaughn AE, Deshmukh M (2008) Glucose metabolism inhibits apoptosis in neurons and cancer cells by redox inactivation of cytochrome c. *Nat Cell Biol* 10:1477–1483.
10. Settergren G, Lindblad BS, Persson B (1976) Cerebral blood flow and exchange of oxygen, glucose, ketone bodies, lactate, pyruvate and amino acids in infants. *Acta Paediatr Scand* 65:343–353.
11. Fox PT, Raichle ME, Mintun MA, Dence C (1988) Nonoxidative glucose consumption during focal physiologic neural activity. *Science* 241:462–464.
12. Vlassenko AG, Rundle MM, Mintun MA (2006) Human brain glucose metabolism may evolve during activation: Findings from a modified FDG PET paradigm. *Neuroimage* 33:1036–1041.
13. Kasischke KA, Vishwasrao HD, Fisher PJ, Zipfel WR, Webb WW (2004) Neural activity triggers neuronal oxidative metabolism followed by astrocytic glycolysis. *Science* 305: 99–103.
14. Pellerin L, Magistretti PJ (1994) Glutamate uptake into astrocytes stimulates aerobic glycolysis: A mechanism coupling neuronal activity to glucose utilization. *Proc Natl Acad Sci USA* 91:10625–10629.
15. McAvoy MP, Ollinger JM, Buckner RL (2001) Cluster size thresholds for assessment of significant activation in fMRI. *Neuroimage* 13:S198.
16. Forman SD, et al. (1995) Improved assessment of significant activation in functional magnetic resonance imaging (fMRI): Use of a cluster-size threshold. *Magn Reson Med* 33:636–647.
17. Raichle ME, Snyder AZ (2007) A default mode of brain function: A brief history of an evolving idea. *Neuroimage* 37:1083–1090, discussion 1097–1099.
18. Buckner RL, Andrews-Hanna JR, Schacter DL (2008) The brain's default network: Anatomy, function, and relevance to disease. *Ann N Y Acad Sci* 1124:1–38.
19. Braver TS, Barch DM (2006) Extracting core components of cognitive control. *Trends Cogn Sci* 10:529–532.
20. Dosenbach NU, Fair DA, Cohen AL, Schlaggar BL, Petersen SE (2008) A dual-networks architecture of top-down control. *Trends Cogn Sci* 12:99–105.
21. Vincent JL, Kahn I, Snyder AZ, Raichle ME, Buckner RL (2008) Evidence for a frontoparietal control system revealed by intrinsic functional connectivity. *J Neurophysiol* 100: 3328–3342.
22. Raichle ME, et al. (2001) A default mode of brain function. *Proc Natl Acad Sci USA* 98: 676–682.
23. Greicius MD, Krasnow B, Reiss AL, Menon V (2003) Functional connectivity in the resting brain: A network analysis of the default mode hypothesis. *Proc Natl Acad Sci USA* 100:253–258.
24. Fox MD, et al. (2005) The human brain is intrinsically organized into dynamic, anticorrelated functional networks. *Proc Natl Acad Sci USA* 102:9673–9678.
25. Fox MD, Raichle ME (2007) Spontaneous fluctuations in brain activity observed with functional magnetic resonance imaging. *Nat Rev Neurosci* 8:700–711.
26. Hagmann P, et al. (2008) Mapping the structural core of human cerebral cortex. *PLoS Biol* 6:e159.
27. Buckner RL, et al. (2009) Cortical hubs revealed by intrinsic functional connectivity: Mapping, assessment of stability, and relation to Alzheimer's disease. *J Neurosci* 29: 1860–1873.
28. Vincent JL, et al. (2006) Coherent spontaneous activity identifies a hippocampal-parietal memory network. *J Neurophysiol* 96:3517–3531.
29. Pellerin L, Magistretti PJ (1996) Excitatory amino acids stimulate aerobic glycolysis in astrocytes via an activation of the Na+/K+ ATPase. *Dev Neurosci* 18:336–342.
30. Magistretti PJ, Chatton JY (2005) Relationship between L-glutamate-regulated intracellular Na+ dynamics and ATP hydrolysis in astrocytes. *J Neural Transm* 112:77–85.
31. Mercer RW, Dunham PB (1981) Membrane-bound ATP fuels the Na/K pump. Studies on membrane-bound glycolytic enzymes on inside-out vesicles from human red cell membranes. *J Gen Physiol* 78:547–568.
32. Okamoto K, Wang W, Rounds J, Chambers EA, Jacobs DO (2001) ATP from glycolysis is required for normal sodium homeostasis in resting fast-twitch rodent skeletal muscle. *Am J Physiol Endocrinol Metab* 281:E479–E488.
33. Campbell JD, Paul RJ (1992) The nature of fuel provision for the Na+,K(+)-ATPase in porcine vascular smooth muscle. *J Physiol* 447:67–82.
34. Wu K, Aoki C, Elste A, Rogalski-Wilk AA, Siekevitz P (1997) The synthesis of ATP by glycolytic enzymes in the postsynaptic density and the effect of endogenously generated nitric oxide. *Proc Natl Acad Sci USA* 94:13273–13278.
35. McGilvery RW, Goldstein GW (1983) *Biochemistry: A Functional Approach* (Saunders, Philadelphia).
36. Azevedo FA, et al. (2009) Equal numbers of neuronal and nonneuronal cells make the human brain an isometrically scaled-up primate brain. *J Comp Neurol* 513:532–541.
37. Kennedy MB (2000) Signal-processing machines at the postsynaptic density. *Science* 290:750–754.
38. Kennedy MJ, Ehlers MD (2006) Organelles and trafficking machinery for postsynaptic plasticity. *Annu Rev Neurosci* 29:325–362.
39. Marder E, Goaillard JM (2006) Variability, compensation and homeostasis in neuron and network function. *Nat Rev Neurosci* 7:563–574.
40. Zhang D, et al. (2009) Na,K-ATPase activity regulates AMPA receptor turnover through proteasome-mediated proteolysis. *J Neurosci* 29:4498–4511.
41. Li Z, Okamoto K, Hayashi Y, Sheng M (2004) The importance of dendritic mitochondria in the morphogenesis and plasticity of spines and synapses. *Cell* 119:873–887.
42. Sheng M, Hoogenraad CC (2007) The postsynaptic architecture of excitatory synapses: A more quantitative view. *Annu Rev Biochem* 76:1.1–1.25.
43. Cai Q, Sheng ZH (2009) Mitochondrial transport and docking in axons. *Exp Neurol* 218:257–267.
44. Pierre K, et al. (2009) Linking supply to demand: The neuronal monocarboxylate transporter MCT2 and the alpha-amino-3-hydroxyl-5-methyl-4-isoxazole-propionic acid receptor GluR2/3 subunit are associated in a common trafficking process. *Eur J Neurosci* 29:1951–1963.

45. Jannière L, et al. (2007) Genetic evidence for a link between glycolysis and DNA replication. *PLoS ONE* 2:e447.
46. DeBerardinis RJ, et al. (2007) Beyond aerobic glycolysis: Transformed cells can engage in glutamine metabolism that exceeds the requirement for protein and nucleotide synthesis. *Proc Natl Acad Sci USA* 104:19345–19350.
47. Gaitonde MK, Jones J, Evans G (1987) Metabolism of glucose into glutamate via the hexose monophosphate shunt and its inhibition by 6-aminonicotinamide in rat brain in vivo. *Proc R Soc Lond B Biol Sci* 231:71–90.
48. Dringen R, Hoepken HH, Minich T, Ruedig C (2007) Pentose phosphate pathway and NADPH metabolism.*Brain Energetics. Integration of Molecular and Cellular Processes, Handbook of Neurochemistry and Molecular Neurobiology*, eds Gibson GE, Dienel GA (Springer, New York), 3rd Ed.
49. Herrero-Mendez A, et al. (2009) The bioenergetic and antioxidant status of neurons is controlled by continuous degradation of a key glycolytic enzyme by APC/C-Cdh1. *Nat Cell Biol* 11:747–752.
50. Altman DI, Perlman JM, Volpe JJ, Powers WJ (1993) Cerebral oxygen metabolism in newborns. *Pediatrics* 92:99–104.
51. Powers WJ, Rosenbaum JL, Dence CS, Markham J, Videen TO (1998) Cerebral glucose transport and metabolism in preterm human infants. *J Cereb Blood Flow Metab* 18: 632–638.
52. Chugani HT, Phelps ME, Mazziotta JC (1987) Positron emission tomography study of human brain functional development. *Ann Neurol* 22:487–497.
53. Elston GN, Oga T, Fujita I (2009) Spinogenesis and pruning scales across functional hierarchies. *J Neurosci* 29:3271–3275.
54. Madsen PL, et al. (1995) Persistent resetting of the cerebral oxygen/glucose uptake ratio by brain activation: Evidence obtained with the Kety-Schmidt technique. *J Cereb Blood Flow Metab* 15:485–491.
55. Tononi G, Cirelli C (2006) Sleep function and synaptic homeostasis. *Sleep Med Rev* 10: 49–62.
56. Vyazovskiy VV, Cirelli C, Pfister-Genskow M, Faraguna U, Tononi G (2008) Molecular and electrophysiological evidence for net synaptic potentiation in wake and depression in sleep. *Nat Neurosci* 11:200–208.
57. Vyazovskiy VV, Cirelli C, Tononi G, Tobler I (2008) Cortical metabolic rates as measured by 2-deoxyglucose-uptake are increased after waking and decreased after sleep in mice. *Brain Res Bull* 75:591–597.
58. Ido Y, Chang K, Williamson JR (2004) NADH augments blood flow in physiologically activated retina and visual cortex. *Proc Natl Acad Sci USA* 101:653–658.
59. Mintun MA, Vlassenko AG, Rundle MM, Raichle ME (2004) Increased lactate/pyruvate ratio augments blood flow in physiologically activated human brain. *Proc Natl Acad Sci USA* 101:659–664.
60. Vlassenko AG, et al. (2010) Spatial correlation between brain aerobic glycolysis and A-beta deposition. *Proc Natl Acad Sci USA*, 10.1073/pnas.1010461107.
61. Buckner RL, et al. (2005) Molecular, structural, and functional characterization of Alzheimer's disease: Evidence for a relationship between default activity, amyloid, and memory. *J Neurosci* 25:7709–7717.
62. Raichle ME, Martin WR, Herscovitch P, Mintun MA, Markham J (1983) Brain blood flow measured with intravenous H2(15)O. II. Implementation and validation. *J Nucl Med* 24:790–798.
63. Mintun MA, Raichle ME, Martin WR, Herscovitch P (1984) Brain oxygen utilization measured with O-15 radiotracers and positron emission tomography. *J Nucl Med* 25: 177–187.
64. Martin WR, Powers WJ, Raichle ME (1987) Cerebral blood volume measured with inhaled C15O and positron emission tomography. *J Cereb Blood Flow Metab* 7:421–426.
65. Lancaster JL, et al. (1995) A modality-independent approach to spatial normalization of tomographic images of the human brain. *Hum Brain Mapp* 3:209–223.
66. Van Essen DC (2005) A Population-Average, Landmark- and Surface-based (PALS) atlas of human cerebral cortex. *Neuroimage* 28:635–662.